

Exact Solutions of Regge-Wheeler Equation and Quasi-Normal Modes of Compact Objects

Plamen P. Fiziev*

Abstract

The well-known Regge-Wheeler equation describes the axial perturbations of Schwarzschild metric in the linear approximation. From a mathematical point of view it presents a particular case of the confluent Heun equation and can be solved exactly, due to recent mathematical developments. We present the basic properties of its general solution. A novel analytical approach and numerical techniques for study the boundary problems which correspond to quasi-normal modes of black holes and other simple models of compact objects are developed.

1 Introduction

In the linear approximation the axial perturbations of Schwarzschild metric of Keplerian mass M are described by the well-known Regge-Wheeler equation [1]:

$$\partial_t^2 \Phi_{s,l} + (-\partial_x^2 + V_{s,l}) \Phi_{s,l} = 0. \quad (1.1)$$

Here $x = r + r_s \ln(r/r_s - 1)$ is the Regge-Wheeler "tortoise" coordinate, $r_s = 2M (= 1)$ is the Schwarzschild radius, and $\Phi_{s,l}(t, r)$ is the radial function for perturbations of spin s and angular momentum $l \geq s$. The corresponding effective potential $V_{s,l}(r)$ reads: $V_{s,l}(r) = (1 - \frac{1}{r}) \left(\frac{l(l+1)}{r^2} + \frac{1-s^2}{r^3} \right)$. The area radius r in it can be expressed explicitly as a function of the variable x using Lambert W-function [2]: $r/r_s = LambertW(e^{x/r_s-1}) + 1$.

The standard ansatz $\Phi_{s,l}(t, r) = R_{\varepsilon,s,l}(r)e^{i\varepsilon t}$ brings us to the stationary problem:

$$\partial_x^2 R_{\varepsilon,s,l} + (\varepsilon^2 - V_{s,l}) R_{\varepsilon,s,l} = 0. \quad (1.2)$$

A large amount of references on this subject can be found in the review articles [3]. There we meet often the statement that the exact solution of the problem is not known. Therefore, quite sophisticated approximate analytical and numerical techniques for solution of physical problems related to Eqs. (1.1), (1.2) were developed in the past. They discovered rich and important mathematical and physical properties of the corresponding problems. Some of them need further justification.

A hint on the class of new mathematical functions, which solve the stationary Regge-Wheeler problem (1.2) is the use of the very time-time component of Schwarzschild metric

*Department of Theoretical Physics, University of Sofia, Boulevard 5 James Bourchier, Sofia 1164, Bulgaria; E-mail: fiziev@phys.uni-sofia.bg

$g_{tt} = 1 - 1/r = g$ as an independent variable, instead of the area-radius r . This transforms the Eq. (1.2) into:

$$\partial_x^2 R_{\varepsilon,s,l} + (\varepsilon^2 - W_{s,l}) R_{\varepsilon,s,l} = 0 \quad (1.3)$$

with the potential $W_{s,l}(g) = l(l+1)g(1-g)^2 + (1-s^2)g(1-g)^3$ which describes anharmonic oscillators of different type, depending on the values of spin: $s = 0$ – for scalar waves, $s = 1$ – for electromagnetic waves, $s = 2$ – for gravitational waves (see Fig. 1).

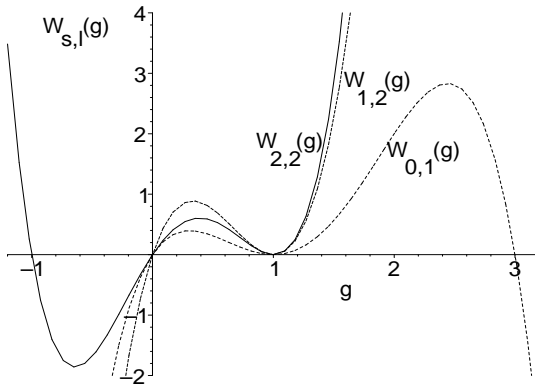


Figure 1: Typical forms of the potentials $W_{s,l}(g)$ for different s, l . The physical domain is $g \in (0, 1)$. The point $g = 0$ represents the Schwarzschild event horizon, the point $g = 1$ – the physical infinity.

This simple observation sheds additional light on the physical content of Eq.(1.2) and yields a better understanding of the qualitative differences and similarities between the perturbations of different spin. In particular, one can see in a more clear way the behavior of the potential, the RW equation and its solutions at infinite space points when these are placed at finite distances, using the variable g .

Here we utilize the form (1.3) of the problem at hand only as a hint on a new direction of mathematical investigation. It is well known that the above polynomial form of the potential $W_{s,l}(g)$ leads to a solution of geodesic equations in Schwarzschild metric in elliptic functions. According to the early article [4], in this case the corresponding Schrödinger like spectral problem can be solved by the method of continuous fractions. This method was developed for the specific RW spectral problem by Leaver [3] and at present is one of the basic methods for finding the QNM spectra.

The modern mathematical development shows that many physical problems, including anharmonic oscillator ones, are solved exactly by Heun's functions [5]. Thus the form of the Eq.(1.3) suggests to describe the exact solution of Regge-Wheeler equation using Heun's functions. We shall show that the Eqs. (1.2), (1.3) can be transformed to a particular case of confluent Heun equation.

The confluent Heun equation of general form is well known and studied in some detail in recent mathematical literature [5]. At present its solutions are more or less well-described special functions, already included in modern computer packages. In particular, the Heun's functions are included in the last version of the widespread computer package Maple 10, which has been used in all original numerical calculations in our article. These

functions present a nontrivial generalization of familiar hypergeometric functions and have much richer and complicated properties, since the Heun equation has one more singular point, than the hypergeometric equation.

In the present article, we give the exact solution of the Regge-Wheeler equation in terms of Heun's functions and apply them for study of different boundary problems in the relativistic theory of gravity.

2 Solutions of Regge-Wheeler Equation

2.1 Local Solutions of Confluent Heun Equation

It is convenient to use the standard variable r for reaching the standard canonical form of the Heun equation of our problem. The explicit form:

$$\frac{d^2 R_{\varepsilon,s,l}}{dr^2} + \frac{1}{r(r-1)} \frac{dR_{\varepsilon,s,l}}{dr} + \frac{\varepsilon^2 r^4 - l(l+1)r^2 + (l(l+1) + s^2 - 1)r + 1 - s^2}{r^2(r-1)^2} R_{\varepsilon,s,l} = 0 \quad (2.1)$$

of Eq. (1.2) shows that it has three singular points: the origin $r = 0$, the horizon $r = 1$ and the infinite point $r = \infty$ [5]. The first two are regular singular points and may be treated on equal terms. The last one is an irregular singular point, obtained as a result of confluence of two regular singular points in the general Heun equation. Hence, we are to consider a specific representative of the class of confluent Heun equations. This circumstance is the source of complicated analytical properties of solutions of the Regge-Wheeler equation, as we shall see below.

For transformation of Eq. (2.1) to a canonical form of the Heun equation [5] :

$$\begin{aligned} \frac{d^2 H}{dr^2} + \left(\alpha + \frac{\beta + 1}{r} + \frac{\gamma + 1}{r-1} \right) \frac{dH}{dr} + \\ \frac{1}{r(r-1)} \left(\left(\delta + \frac{1}{2}\alpha(\beta + \gamma + 2) \right) r + \eta + \frac{\beta}{2} + \frac{1}{2}(\gamma - \alpha)(\beta + 1) \right) H = 0 \end{aligned} \quad (2.2)$$

one may use the ansatz $R_{\varepsilon,s,l}(r) = r^{s+1}(r-1)^{i\varepsilon} e^{i\varepsilon r} H(r)$. It yields the following specific parameters: $\alpha = 2i\varepsilon$, $\beta = 2s$, $\gamma = 2i\varepsilon$, $\delta = 2\varepsilon^2$, $\eta = s^2 - l(l+1)$.

There exist several substitutions of that kind. All they transform Eq. (2.1) to the same form (2.2), but with different coefficients, for example, with all possible combinations of the signs of the coefficients α , β and γ . The corresponding solutions of equations (2.2), with different coefficients, are related by simple transformations, described in literature [5]. It is useful to know all sets of such transformations and corresponding parameters. In some cases this permits us to construct two independent solutions of stationary Regge-Wheeler equation (1.2), using the basic standard canonical solution of confluent Heun equation (2.2)¹:

$$HeunC(\alpha, \beta, \gamma, \delta, \eta, r), \quad (2.3)$$

which is defined by the convergent Taylor series expansion around the origin $r = 0$ and

¹In present article we apply the notations for Heun's functions, which are used in Maple 10.

normalization:

$$HeunC(\alpha, \beta, \gamma, \delta, \eta, 0) = 1, \quad (2.4a)$$

$$\frac{d}{dr}HeunC(\alpha, \beta, \gamma, \delta, \eta, 0) = \frac{1}{2} \frac{\beta(-\alpha + \gamma + 1) - \alpha + \gamma + 2\eta}{\beta + 1}. \quad (2.4b)$$

The Taylor series expansion of the standard canonical solution (2.3) with respect to the independent variable r is obtained using the known three-terms recurrence relation [5] and initial conditions (2.4).

It is not excluded that some specific sets of parameters $\alpha, \beta, \gamma, \delta, \eta$ may not yield well defined canonical solutions (2.3) of the confluent Heun equation (2.2). This indeed happens in our problem, since in it $s \in \mathbb{Z}$ and $s \geq 0$. As a result, for example, solutions $HeunC(\alpha, \beta, \gamma, \delta, \eta, r)$ with $\beta = -2s$ are not well defined, because the denominator of the coefficients in Taylor series expansion includes products of form $\beta(\beta+1)\dots(\beta+N)$, $N \in \mathbb{Z}^+$.

One can go outside the domain of convergence of the Taylor series expansion – the open unit disk in \mathbb{C}_r , centered at the origin, using an analytical continuation in this complex plain. The relations between Heun functions of different values of parameters and arguments, described in the mathematical literature [5], are useful for this purpose, too.

Using these techniques we obtain the following local solutions of the confluent Heun equation (2.2):

1. Around the singular point $r = 0$ there exist two independent local solutions $H_{\varepsilon, s, l}^{(0)\pm}(r)$ with asymptotics:

$$H_{\varepsilon, s, l}^{(0)+}(r) \sim \frac{1}{r^{2s}}, \quad H_{\varepsilon, s, l}^{(0)-}(r) \sim 1. \quad (2.5)$$

The second one is the standard canonical solution:

$$H_{\varepsilon, s, l}^{(0)-}(r) = HeunC(2i\varepsilon, 2s, 2i\varepsilon, 2\varepsilon^2, s^2 - l(l+1), r), \quad (2.6)$$

which has convergent Taylor series expansion around the origin $r = 0$. This solution is the only one, which is finite at the point $r = 0$. It is normalized according to the relations:

$$H_{\varepsilon, s, l}^{(0)-}(0) = HeunC(2i\varepsilon, 2s, 2i\varepsilon, 2\varepsilon^2, s^2 - l(l+1), 0) = 1, \quad (2.7a)$$

$$\frac{d}{dr}H_{\varepsilon, s, l}^{(0)-}(0) = \frac{d}{dr}HeunC(2i\varepsilon, 2s, 2i\varepsilon, 2\varepsilon^2, s^2 - l(l+1), 0) = \frac{s(s+1) - l(l+1)}{2s+1}. \quad (2.7b)$$

In the general case, the solutions of this type diverge at the horizon $r = 1$. There exist a countable number of such solutions which are finite simultaneously at the origin and at the horizon. Considering them, one can derive a discrete spectrum of values $\varepsilon_{n, s, l}$ for the boundary problem on the interval $r \in [0, 1]$. To the best of our knowledge, this boundary problem has not attracted attention in the existing physical applications and its spectrum is not known at present, although it must be interesting for the study of the interior of Schwarzschild black holes². Indeed, these solutions are obviously square integrable functions on the interval $r \in [0, 1]$. If they will be proven to form a complete

²Note that in this domain the variable r plays the role of a time variable and the dependence of the former stationary solutions on the new space variable t is described by the simple exponential factor $e^{i\varepsilon t}$.

set in the corresponding functional space, these solutions will present a natural basis of *normal modes* for a well defined expansion of any small perturbation of the metric in the interior of the black hole. Therefore these solutions seem to deserve a separate consideration.

The first independent local solution in Eqs. (2.5) – $H_{\varepsilon,s,l}^{(0)+}(r)$ cannot be described by standard solution (2.3) of the confluent Heun equation for any set of parameters. Since $b = 2s$ is positive integer, the second solution includes the $\ln r$ terms [5]. It is analogous to the corresponding case of solutions of confluent hypergeometric equation, but we were not able to find more information about this solution in the available mathematical literature. Taking into account the well-known example of hydrogen atom, described by confluent hypergeometric functions, one can think that this solution may not play an essential role in most of the physical applications. Nevertheless, for completeness we shall add formally this solution to our list, using for it the notation $H_{\varepsilon,s,l}^{(0)+}(r)$.

2. We have two independent local solutions of the Heun confluent equation (2.2):

$$H_{\varepsilon,s,l}^{(1)+}(r) = \text{HeunC}(-2i\varepsilon, +2i\varepsilon, 2s, -2\varepsilon^2, 2\varepsilon^2 + s^2 - l(l+1), 1-r), \quad (2.8a)$$

$$H_{\varepsilon,s,l}^{(1)-}(r) = (r-1)^{-2i\varepsilon} \text{HeunC}(-2i\varepsilon, -2i\varepsilon, 2s, -2\varepsilon^2, 2\varepsilon^2 + s^2 - l(l+1), 1-r). \quad (2.8b)$$

The functions $H_{\varepsilon,s,l}^{(1)+}(r)$ and $(r-1)^{2i\varepsilon} H_{\varepsilon,s,l}^{(1)-}(r)$ have convergent Taylor series expansion around the second singular point – the horizon $r = 1$. They are normalized in the following way:

$$\left. \begin{array}{l} H_{\varepsilon,s,l}^{(1)+}(r) \\ (r-1)^{2i\varepsilon} H_{\varepsilon,s,l}^{(1)-}(r) \end{array} \right|_{r=1} \quad \left. \begin{array}{l} \\ \end{array} \right\} = 1, \quad (2.9a)$$

$$\left. \begin{array}{l} \frac{d}{dr} H_{\varepsilon,s,l}^{(1)+}(r) \\ \frac{d}{dr} \left((r-1)^{2i\varepsilon} H_{\varepsilon,s,l}^{(1)-}(r) \right) \end{array} \right|_{r=1} \quad \left. \begin{array}{l} \\ \end{array} \right\} = \frac{2\varepsilon^2(1 \mp 1) \pm 2i\varepsilon s + i\varepsilon(1 \pm 1) + s(s+1) - l(l+1)}{\pm 2i\varepsilon + 1}. \quad (2.9b)$$

The first solution (2.8a) is the only one which is regular at the horizon $r = 1$. In general case, the two solutions (2.8) diverge at both the origin $r = 0$ and the infinity $r = \infty$. Using them one can formulate the corresponding two-point boundary problems and find their discrete spectra. We shall consider some of them in the next sections.

3. Using known three-term recurrence relations for the coefficients a_ν^\pm , one is able to construct two asymptotics-series solutions around the infinite irregular singular point $r = \infty$ [5]:

$$H_{\varepsilon,s,l}^{(\infty)+}(r) \sim r^{-s-1} e^{-2i\varepsilon(r+\ln r)} \sum_{\nu \geq 0} \frac{a_\nu^+}{r^\nu}, \quad a_0^+ = 1 \quad (2.10a)$$

$$H_{\varepsilon,s,l}^{(\infty)-}(r) \sim r^{-s-1} \sum_{\nu \geq 0} \frac{a_\nu^-}{r^\nu}, \quad a_0^- = 1; \quad (2.10b)$$

They are valid in the complex domain

$$-\frac{\pi}{2} - l(l+1) + s^2 \leq \arg(r) + \arg(\varepsilon) \leq 3\frac{\pi}{2} + l(l+1) - s^2, \quad (2.11)$$

see the articles by A. Decarreau et al. in [5], where one can find the restrictions of this kind for the general case of the confluent Heun equation. In our particular problem Eq. (2.11)

leads to inessential restrictions on the variables in the complex plain \mathbb{C} , since the length of the admissible interval of arguments $\arg(r)$ and $\arg(\varepsilon)$ is $2\pi + 2l(l+1) - 2s^2 \geq 2(\pi + s) \geq 2\pi$ for $l \geq s \geq 0$.

Unfortunately, the transition coefficients between the three sets of local solutions (2.6), (2.8) and (2.10) are not known at present. The only available information is negative: these coefficients cannot be expressed even in terms of hypergeometric functions [5]. The same transition coefficients relate the corresponding local solutions of the Regge-Wheeler equation, see below.

2.2 Local Solutions of Regge-Wheeler Equation

In accord with the above local solutions of the Heun equation (2.2), we obtain the following three sets of independent local solutions of the Regge-Wheeler equation (1.1):

$$\Phi_{\varepsilon,s,l}^{(0)\pm}(t, r) = e^{i\varepsilon t} R_{\varepsilon,s,l}^{(0)\pm}(r), \quad (2.12a)$$

$$R_{\varepsilon,s,l}^{(0)\pm}(r) = r^{s+1} e^{i\varepsilon r + i\varepsilon \ln(1-r)} \begin{cases} H_{\varepsilon,s,l}^{(0)+}(r), \\ \text{HeunC}(2i\varepsilon, 2s, 2i\varepsilon, 2\varepsilon^2, s^2 - l(l+1), r); \end{cases} \quad (2.12b)$$

$$\Phi_{\varepsilon,s,l}^{(1)\pm}(t, r) = e^{i\varepsilon t} R_{\varepsilon,s,l}^{(1)\pm}(r), \quad (2.13a)$$

$$R_{\varepsilon,s,l}^{(1)\pm}(r) = r^{s+1} e^{i\varepsilon r \pm i\varepsilon \ln(r-1)} \text{HeunC}(-2i\varepsilon, \pm 2i\varepsilon, 2s, -2\varepsilon^2, 2\varepsilon^2 + s^2 - l(l+1), 1-r); \quad (2.13b)$$

$$\Phi_{\varepsilon,s,l}^{(\infty)\pm}(t, r) = e^{i\varepsilon t} R_{\varepsilon,s,l}^{(\infty)\pm}(r), \quad (2.14a)$$

$$R_{\varepsilon,s,l}^{(\infty)\pm}(r) \sim e^{\mp i\varepsilon r - i\varepsilon \ln r} \sum_{\nu \geq 0} \frac{a_\nu^\pm}{r^\nu}, \quad a_0^\pm = 1. \quad (2.14b)$$

They are correspondingly defined in domains around the three singular points of the problem: the origin $r = 0$, horizon $r = 1$ and infinity $r = \infty$, as pointed in the upper indices of our notation. Any other radial function $R_{\varepsilon,s,l}(r)$, being solution of the stationary Regge-Wheeler equation (1.2), can be represented locally in the form of a linear combination:

$$R_{\varepsilon,s,l}(r) = C_{X+} R_{\varepsilon,s,l}^{(X)+}(r) + C_{X-} R_{\varepsilon,s,l}^{(X)-}(r), \quad (2.15)$$

where $C_{X\pm}$ are proper constants and $X = 0, 1, \infty$ indicates the corresponding singular point.

For fixed values of the parameters ε, s, l each of the three sets (2.12), (2.13) and (2.14) includes two independent local solutions of the stationary Regge-Wheeler equation (1.2). Hence, in the corresponding common domains of validity of these solutions one obtains:

$$R_{\varepsilon,s,l}^{(X)\pm}(r) = \Gamma_{Y+}^{X\pm}(\varepsilon, s, l) R_{\varepsilon,s,l}^{(Y)+}(r) + \Gamma_{Y-}^{X\pm}(\varepsilon, s, l) R_{\varepsilon,s,l}^{(Y)-}(r), \quad (2.16)$$

expanding one set of local solutions onto another. The main obstacle for analytical treatment of different interesting problems related to the Regge-Wheeler equation is that the transition coefficients $\Gamma_{Y\pm}^{X\pm}(\varepsilon, s, l)$ for $X, Y = 0, 1, \infty; X \neq Y$ are unknown explicitly.

2.3 Some Basic Properties of the Local Solutions of Regge-Wheeler Equation

2.3.1 In-Out Properties of the Local Solutions

Taking into account the relation (2.4a), one easily obtains directions of spreading of the corresponding waves described by local solutions (2.12a), (2.13a) and (2.14a) in the vicinity of the corresponding singular points X when the time t increases³. These "in" and "out" properties of local solutions are illustrated by the graphical schemes, shown in Table 1:

$\Phi_{\varepsilon,s,l}^{(0)+}(t,r) : 0 \leftarrow$	$\Phi_{\varepsilon,s,l}^{(0)-}(t,r) : 0 \rightarrow$
$\Phi_{\varepsilon,s,l}^{(1)+}(t,r) : 1 \leftarrow$	$\Phi_{\varepsilon,s,l}^{(1)-}(t,r) : 1 \rightarrow$
$\Phi_{\varepsilon,s,l}^{(\infty)+}(t,r) : \rightarrow \infty$	$\Phi_{\varepsilon,s,l}^{(\infty)-}(t,r) : \leftarrow \infty$

Table 1: In-Out properties of local solutions

Thus, we see that according to our conventions, the local solutions $\Phi_{\varepsilon,s,l}^{(X)+}$ describe waves going in the singular point X and the local solutions $\Phi_{\varepsilon,s,l}^{(X)-}$ describe waves going out of singular point X .

2.3.2 Time and Space Limits of Local Solutions for Complex Values of ε

In general, we have to consider complex valued $\varepsilon = \varepsilon_R + i\varepsilon_I \in \mathbb{C}_\varepsilon$. Since in the Regge-Wheeler equation only the squared quantity ε emerges, without loss of generality one can accept conventionally that its real part is nonnegative: $\varepsilon_R \geq 0$ ⁴.

The local solutions (2.12a), (2.13a) and (2.14a) have the following obvious time-limits:

$$\lim_{t \rightarrow +\infty} |\Phi_{\varepsilon,s,l}^{(X)\pm}(t,r)| = \begin{cases} 0 \quad \forall r, & \text{if } \varepsilon_I > 0 \text{ and } |R_{\varepsilon,s,l}^{(X)\pm}(r)| \neq \infty; \\ |R_{\varepsilon,s,l}^{(X)\pm}(r)|, & \text{if } \varepsilon_I = 0; \\ \infty \quad \forall r, & \text{if } \varepsilon_I < 0 \text{ and } |R_{\varepsilon,s,l}^{(X)\pm}(r)| \neq 0. \end{cases} \quad (2.17)$$

Hence, from a physical point of view we have to work only with $\varepsilon_I \geq 0$ [1], because the solutions with $\varepsilon_I < 0$ are certainly unstable and, therefore, nonphysical. Then, for finite values of t in general we obtain the following space limits of the local solutions:

$$\lim_{r \rightarrow X} |\Phi_{\varepsilon,s,l}^{(X)+}(t,r)| = \infty, \quad (2.18a)$$

$$\lim_{r \rightarrow X} |\Phi_{\varepsilon,s,l}^{(X)-}(t,r)| = 0. \quad (2.18b)$$

These need some justification for different singular points:

³The only still unstudied solution $H_{\varepsilon,s,l}^{(0)+}(r)$ has to be chosen in a proper way to insure the fulfilment of our "in-out" conventions. This requirement fixes the solution $H_{\varepsilon,s,l}^{(0)+}(r)$ up to inessential normalization.

⁴In the case $\varepsilon_R = 0$, we may have "pseudo" waves. The corresponding solutions do not oscillate.

1. The limits (2.18) of local solutions around the origin $r=0$ are valid for $s>0$ and on any contour to this point in the complex plane \mathbb{C}_r . For $s=0$ the limit (2.18b) equals 1.
2. Around the horizon $r = 1$ the limits (2.18) of local solutions are valid for all real values of $s \geq 0$ and on any contour to this point in the complex plane \mathbb{C}_r .
3. The behavior of limits (2.18) of local solutions in the complex plane \mathbb{C}_r around the infinite irregular singular point $r = \infty$ is more complicated and depends on the direction of the contour which approaches this point. This reflects the well-known Stocks phenomenon (see references in [3, 5]), and is related with the multiplier

$$e^{\mp i\varepsilon r - i\varepsilon \ln r} = e^{i(\alpha \mp |\varepsilon| |r| \cos(\arg(r) + \arg(\varepsilon)))} e^{\pm |\varepsilon| |r| \sin(\arg(r) + \arg(\varepsilon)) + |\varepsilon| \ln |r| \cos(\arg(\varepsilon))}$$

in (2.14b). Thus we see that

$$|R_{\varepsilon,s,l}^{(\infty)\pm}(r)| \sim e^{\pm |\varepsilon| |r| \sin(\arg(r) + \arg(\varepsilon)) + |\varepsilon| \ln |r| \cos(\arg(\varepsilon))}, \quad (2.19)$$

and in the case $|\varepsilon| > 0$ we obtain:

$$\lim_{|r| \rightarrow \infty} |R_{\varepsilon,s,l}^{(\infty)+}(r)| = \begin{cases} \infty, & \text{if } \arg(r) + \arg(\varepsilon) \in (0, \pi) \bmod 2\pi; \\ 0, & \text{if } \arg(r) + \arg(\varepsilon) \in (-\pi, 0) \bmod 2\pi. \end{cases} \quad (2.20a)$$

$$\lim_{|r| \rightarrow \infty} |R_{\varepsilon,s,l}^{(\infty)-}(r)| = \begin{cases} 0, & \text{if } \arg(r) + \arg(\varepsilon) \in (0, \pi) \bmod 2\pi; \\ \infty, & \text{if } \arg(r) + \arg(\varepsilon) \in (-\pi, 0) \bmod 2\pi. \end{cases} \quad (2.20b)$$

In the case $|\varepsilon| = 0$ we obtain:

$$\lim_{|r| \rightarrow \infty} |R_{\varepsilon,s,l}^{(\infty)\pm}(r)| = 1. \quad (2.21)$$

Relations (2.20) and (2.21) justify the exact behavior of local solutions (2.14), when one approaches the infinite singular point from different directions in the complex plain \mathbb{C}_r . They give precise meaning of limits (2.18) for $X = \infty$. These relations will play an important role in our novel approach to different spectra of the corresponding two-points boundary problems related to the Regge-Wheeler equation.

3 Two-Point Boundary Problems

3.1 General Description and Symbols of Two-Point Boundary Problems for Regge-Wheeler Equation

The two-singular-point boundary problems can be defined on the *real* intervals which contain only two singular end-points and have no other singular points inside. It is possible to consider regular-singular two-point boundary problems too. In this case, one end of the interval is a singular point and the another is a regular point supplied with some standard boundary condition (for example – with Dirichlet's boundary condition, see below). Different boundary conditions correspond to different physical problems described by the same differential equation.

One can find the general definition of a stationary two-singular-point boundary problem in the book by Slavyanov and Lay in [5]. For our problem we need some natural

generalization of this definition which includes not only the case of solutions, which are finite at both singular points. Following the physical traditions (see articles [3]), we use as a basis of such a definition the in-out properties of the time-dependent solutions of the Regge-Wheeler equation, considered in the previous Section. Since we have established the one-to-one correspondence between these properties and the corresponding space limits (2.18) on the *real* axes \mathbb{R}_r , we can reformulate the definition using only the solutions of the stationary Regge-Wheeler equation (1.2) in the spirit of the book by Slavyanov and Lay.

All two-points boundary problems can be formulated using proper constraints on the transition coefficients $\Gamma_{Y\pm}^{X\pm}(\varepsilon, s, l)$ in relations (2.16). This way one obtains equations for finding of corresponding discrete spectra of (possibly complex) values of frequencies ε .

3.2 Two-Singular-Point Problems on the interval $(1, \infty)$

This interval corresponds to the outer domain of Schwarzschild black holes, where the eventual observer lives. Therefore, it is most important from a physical point of view and, correspondingly, most well studied at present. Nevertheless, even for this interval much further work remains to be done.

3.2.1 Quasi-Normal Modes

We start the illustration of the general statements, made in previous Section, with the most well studied at present example of quasi-normal modes (QNM) of Schwarzschild black holes [3], as a specific two-singular-point boundary problem on the interval $(1, \infty)$. Using the graphical scheme, shown in Table 1, we can symbolically write down relation (2.16) in terms of time dependent solutions of the Regge-Wheeler equation as follows:

$$\{1 \leftarrow\} = \Gamma_{\infty+}^{1+}(\varepsilon, s, l)\{\rightarrow \infty\} + \Gamma_{\infty-}^{1+}(\varepsilon, s, l)\{\leftarrow \infty\}. \quad (3.1)$$

By definition, for QNM we have no outgoing waves from the infinite point [3], i.e.

$$\Gamma_{\infty-}^{1+}(\varepsilon, s, l) = 0 \Rightarrow \varepsilon = \varepsilon(n, s, l), \quad n = 0, 1, 2, \dots \quad (3.2)$$

This equation generates the spectrum of QNM. For the above values of ε Eq. (2.16) reads:

$$R_{\varepsilon(n,s,l),s,l}^{(1)+}(r) = \Gamma_{\infty+}^{1+}(\varepsilon(n, s, l), s, l) R_{\varepsilon(n,s,l),s,l}^{(\infty)+}(r). \quad (3.3)$$

We can simplify significantly the notation if we introduce the symbol " $1 \smile \infty$ " for this two-point boundary problem. It reflects symbolically the properties (2.18) of its solutions which enter into relation (3.3). Accordingly, we denote by $\Phi_{1 \smile \infty}(t, r|n, s, l) = e^{i\varepsilon_{1 \smile \infty}(n, s, l)t} R_{1 \smile \infty}(r|n, s, l)$ and $R_{1 \smile \infty}(r|n, s, l) = R_{\varepsilon(n,s,l),s,l}^{(1)+}(r)$ the solutions of this boundary problem, and by $\varepsilon_{1 \smile \infty}(n, s, l)$, the corresponding eigenvalues.

3.2.2 Left Mixed Modes

Under the condition

$$\Gamma_{\infty+}^{1+}(\varepsilon, s, l) = 0 \Rightarrow \varepsilon = \varepsilon_{1 \smile \infty}(n, s, l), \quad n = 0, 1, 2, \dots; \quad (3.4)$$

we obtain the spectrum of the waves, going left from infinity to horizon $r = 1$ without reflection – left mixed modes (LMM)⁵. Due to Eq. (2.18) we use for them the symbol $1 \curvearrowleft \infty$.

Considering the equation

$$\{1 \rightarrow\} = \Gamma_{\infty+}^1(\varepsilon, s, l) \{\rightarrow \infty\} + \Gamma_{\infty-}^1(\varepsilon, s, l) \{\leftarrow \infty\} \quad (3.5)$$

we can introduce two more types of modes of Schwarzschild black holes:

3.2.3 Normal Modes

The equation

$$\Gamma_{\infty+}^1(\varepsilon, s, l) = 0 \Rightarrow \varepsilon = \varepsilon_{1 \curvearrowleft \infty}(n, s, l), \quad n = 0, 1, 2, \dots; \quad (3.6)$$

defines the spectrum of normal modes (NM) on the interval $(1, \infty)$, which are important for considerations of the stability of Schwarzschild black holes. For obvious reasons, related once more to Eq. (2.18), we use for them the symbol $1 \curvearrowleft \infty$.

3.2.4 Right Mixed Modes

Finally, the equation

$$\Gamma_{\infty-}^1(\varepsilon, s, l) = 0 \Rightarrow \varepsilon = \varepsilon_{1 \curvearrowright \infty}(n, s, l), \quad n = 0, 1, 2, \dots; \quad (3.7)$$

defines the spectrum of the waves, going right from the horizon $r = 1$ to infinity without reflection – right mixed modes (RMM). Due to Eq. (2.18) we use for them the symbol $1 \curvearrowright \infty$.

3.3 Two-Singular-Point Problems on the intervals (X, Y)

The generalization of the previous consideration for any real interval (X, Y) with singular ends $X < Y$ and without other singular points in it is obvious. One can introduce the corresponding:

a) Quasi-normal modes: $\Phi_{X \curvearrowleft Y}(t, r|n, s, l) = e^{i\varepsilon_{X \curvearrowleft Y}(n, s, l)t} R_{X \curvearrowleft Y}(r|n, s, l)$ – the solutions of the boundary problem with eigenvalues $\varepsilon_{X \curvearrowleft Y}(n, s, l)$ defined by the equation:

$$\Gamma_{Y-}^{X+}(\varepsilon, s, l) = 0 \Rightarrow \varepsilon = \varepsilon_{X \curvearrowleft Y}(n, s, l), \quad n = 0, 1, 2, \dots. \quad (3.8)$$

b) Left mixed modes: $\Phi_{X \curvearrowleft Y}(t, r|n, s, l) = e^{i\varepsilon_{X \curvearrowleft Y}(n, s, l)t} R_{X \curvearrowleft Y}(r|n, s, l)$ – the solutions with eigenvalues $\varepsilon_{X \curvearrowleft Y}(n, s, l)$ defined by the equation:

$$\Gamma_{Y+}^{X+}(\varepsilon, s, l) = 0 \Rightarrow \varepsilon = \varepsilon_{X \curvearrowleft Y}(n, s, l), \quad n = 0, 1, 2, \dots. \quad (3.9)$$

c) Normal Modes: $\Phi_{X \curvearrowleft Y}(t, r|n, s, l) = e^{i\varepsilon_{X \curvearrowleft Y}(n, s, l)t} R_{X \curvearrowleft Y}(r|n, s, l)$ – the solutions with eigenvalues $\varepsilon_{X \curvearrowleft Y}(n, s, l)$ defined by the equation:

$$\Gamma_{Y+}^{X-}(\varepsilon, s, l) = 0 \Rightarrow \varepsilon = \varepsilon_{X \curvearrowleft Y}(n, s, l), \quad n = 0, 1, 2, \dots. \quad (3.10)$$

⁵We use the term "mixed modes" for indication of the following obvious property of these solutions: Their boundary conditions at the two end points of the corresponding interval are of different type, in the sense of Eq. (2.18).

d) Right mixed modes: $\Phi_{X \sim Y}(t, r|n, s, l) = e^{i\varepsilon_{X \sim Y}(n, s, l)t} R_{X \sim Y}(r|n, s, l)$ – the solutions with eigenvalues $\varepsilon_{X \sim Y}(n, s, l)$, defined by equation:

$$\Gamma_{Y-}^{X-}(\varepsilon, s, l) = 0 \Rightarrow \varepsilon = \varepsilon_{X \sim Y}(n, s, l), \quad n = 0, 1, 2, \dots \quad (3.11)$$

To the best of our knowledge, all spectra of Schwarzschild black hole two-point boundary problems on the intervals $(X, Y) \neq (1, \infty)$ at present are unknown both analytically and numerically. Much better is the situation in the case of the interval $(1, \infty)$: the spectrum of QNM is known in detail, both numerically and analytically [3], although no exact explicit expressions have been obtained up to now. In addition, in this case we have some qualitative studies of the spectrum of normal modes [6].

3.4 Regular-Singular-Two-Point Boundary Problems

3.4.1 Formulation of the Problem and Notations

These two-point boundary problems for the Regge-Wheeler equation (1.1) are related to models of heavy compact objects which are essentially different from a black hole model. The problem of finding the corresponding spectra in the *simple* mathematical formulation, considered below, seems to be new and even not posed in the existing physical literature.

In the present section we consider a one-parameter family of real intervals $(r_*, \infty) \subset (1, \infty)$. The left end of the interval is an arbitrary *regular* point $r_* \in (1, \infty)$ of Eq. (1.2). We pose Dirichlet's boundary condition at this end:

$$\Phi_{\varepsilon, s, l}(t, r_*) = 0. \quad (3.12)$$

Physically, this means that the waves are experiencing a *total* reflection at the spherical surface with the area radius $r = r_* > 1$, instead of going freely through it without any reflection, as in the case of black holes. We have to mention that Dirichlet's boundary condition at the cosmological horizon has been used recently for QNM of AdS black holes in the article [8].

One can consider this surface as a boundary of some *massive* spherically symmetric body. Owing to the Birkhoff theorem, in general relativity the gravitational field of any massive body with Keplerian mass M outside the radius r_* coincides with the corresponding field of a black hole. Hence, the spreading of the waves in the outer domain of the massive body is governed by the Regge-Wheeler equation (1.1), too, but the boundary conditions must be different. The corresponding effective potential $V_{s, l}(r)$ in the Regge-Wheeler equation (1.1) is illustrated in Fig. 2.

There exists a large amount of articles on QNM of relativistic stars [3, 9], both stationary and rotating. At present, this field is well studied in detail. It is known that, in general, the interior of the stars may play a complicated role in the polar oscillations of fields of different spin outside the star. Some details are still an open problem, because the relativistic equation of state of matter is not precisely known for the real case of very high pressures in the compact relativistic stars, for example, in neutron stars.

For axial perturbations of metric the situation is different: axial perturbations do not induce a motion of the star matter and experience only a potential scattering, as in the case of Schwarzschild black holes [3]. This is a physical reason for our simple model of axial perturbations of gravitational field of compact objects.

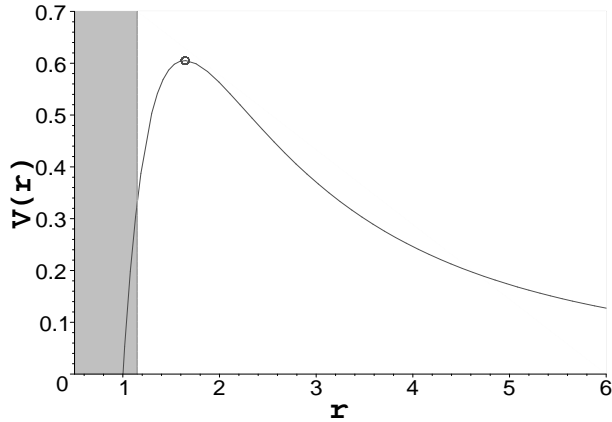


Figure 2: The potential $V_{s,l}(r)$ for $s = 2$, $l = 2$. The small circle marks the place of its maximum (here and at all figures hereafter). The shadowed domain marks the area, which is forbidden for spreading of waves. Its right edge is at the point r_* . The point $r = 1$ presents the event horizon.

In this model, we avoid all complicated problems related to the body's interior, replacing them with the simple boundary condition (3.12). It can be thought as idealization, which describes a proper limiting case of problems related to real bodies. It is obvious that this idealization is opposite to the Schwarzschild black hole model. If there exist a conserved current in the problem at hand, one can expect that the corresponding eigenvalues for real static spherically symmetric objects will be placed between the corresponding eigenvalues of black holes and the eigenvalues of the simple model of massive compact objects, we study here for the first time. Unfortunately, such simple guess turns to be incorrect, because the current in the RW problem with complex eigenvalues ε is not conserved and has quite nontrivial properties, see the Appendix.

In general, one can try to consider two different boundary problems:

- a) Quasi-normal modes of massive compact objects with the spectrum $\varepsilon_{r_* \rightarrow \infty}(n, s, l)$:
 $\Phi_{r_* \rightarrow \infty}(t, r|n, s, l) = e^{i\varepsilon_{r_* \rightarrow \infty}(n, s, l)t} R_{r_* \rightarrow \infty}(r|n, s, l)$, $n = 0, 1, 2, \dots$.
- b) Normal modes of massive compact objects with the spectrum $\varepsilon_{r_* \rightarrow \infty}(n, s, l)$:
 $\Phi_{r_* \rightarrow \infty}(t, r|n, s, l) = e^{i\varepsilon_{r_* \rightarrow \infty}(n, s, l)t} R_{r_* \rightarrow \infty}(r|n, s, l)$, $n = 0, 1, 2, \dots$.

Here we use the symbols $r_* \rightarrow \infty$ and $r_* \bullet \infty$ for QNM and NM in the exterior domain of compact massive objects. In these symbols the sign " $r_* \bullet$ " denotes the spherically symmetric compact object with the boundary of the area radius r_* . The tail denotes the corresponding perturbation mode in accord with the properties described by Eq. (2.18)⁶.

Using the properties of the complex current in RW problem one can prove that NM do not exist under Dirichlet's boundary condition (3.12), see the Appendix. This is well understandable from physical point of view, since in the problem at hand we have no absorbtion of the waves, but a total reflection, creation and emission to space infinity.

⁶From a pure mathematical point of view it is possible to consider analogous modes on intervals (r_*, X) with $X = 1$, $r_* \in (0, 1)$ and $X = 1$, $r_* \in (1, \infty)$, or $X = 0$, $r_* \in (0, 1)$ and even $X = 0$, $r_* \in (-\infty, 0)$, using symbols like $r_* \bullet X$ and $r_* \bullet X$ for the corresponding QNM and NM. Since the physical meaning of such modes is not clear, we will ignore them in the present article.

3.4.2 The Equation for the Discrete Spectrum of QNM

Let us consider solutions of the Regge-Wheeler equation $\Phi_{\varepsilon,s,l}^{r_*}(t, r)$ on the interval (r_*, ∞) , which obey the boundary condition (3.12). Making use of solutions (2.13b) of the stationary equation (1.2), we can represent the solutions $\Phi_{\varepsilon,s,l}^{r_*}(t, r)$ in the following determinant-form:

$$\Phi_{\varepsilon,s,l}^{r_*}(t, r) = e^{i\varepsilon t} \begin{vmatrix} R_{\varepsilon,s,l}^{(1)+}(r) & R_{\varepsilon,s,l}^{(1)-}(r) \\ R_{\varepsilon,s,l}^{(1)+}(r_*) & R_{\varepsilon,s,l}^{(1)-}(r_*) \end{vmatrix} = R_{\varepsilon,s,l}^{(1)-}(r_*) \Phi_{\varepsilon,s,l}^{(1)+}(t, r) - R_{\varepsilon,s,l}^{(1)+}(r_*) \Phi_{\varepsilon,s,l}^{(1)-}(t, r). \quad (3.13)$$

Their expansion on the basis of solutions (2.14), represented in the symbolic form reads:

$$\Phi_{\varepsilon,s,l}^{r_*}(t, r) = \Gamma_{\infty+}^{r_*}(\varepsilon, s, l) \{ \rightarrow \infty \} + \Gamma_{\infty-}^{r_*}(\varepsilon, s, l) \{ \leftarrow \infty \}, \quad (3.14)$$

where $\Gamma_{\infty\pm}^{r_*}(\varepsilon, s, l)$ are proper coefficients. It is obvious that the spectrum of QNM is defined by the following equation:

$$\Gamma_{\infty-}^{r_*}(\varepsilon, s, l) = 0 \Rightarrow \varepsilon_{r_* \rightarrow \infty}(n, s, l), \quad n = 0, 1, 2, \dots \quad (3.15)$$

Now one can use relations (2.15) and (2.16) to obtain:

$$\Gamma_{\infty\pm}^{r_*}(\varepsilon, s, l) = \Gamma_{\infty\pm}^1(\varepsilon, s, l) R_{\varepsilon,s,l}^{(1)-}(r_*) - \Gamma_{\infty\pm}^1(\varepsilon, s, l) R_{\varepsilon,s,l}^{(1)+}(r_*), \quad (3.16)$$

and to represent Eq. (3.15) in the form:

$$\frac{\Gamma_{\infty-}^1(\varepsilon, s, l)}{\Gamma_{\infty+}^1(\varepsilon, s, l)} = \frac{R_{\varepsilon,s,l}^{(1)+}(r_*)}{R_{\varepsilon,s,l}^{(1)-}(r_*)} = e^{2i\varepsilon \ln(r_* - 1)} \frac{HeunC(-2i\varepsilon, +2i\varepsilon, 2s, -2\varepsilon^2, 2\varepsilon^2 + s^2 - l(l+1), 1 - r_*)}{HeunC(-2i\varepsilon, -2i\varepsilon, 2s, -2\varepsilon^2, 2\varepsilon^2 + s^2 - l(l+1), 1 - r_*)}. \quad (3.17)$$

Here we have used the relations (2.13b), too. Relation (3.17) present the final form of the equation for the spectrum of QNM in our simple model of massive compact bodies.

3.4.3 Some General Properties of Trajectories of QNM Eigenvalues $\varepsilon_{r_* \rightarrow \infty}(n, s, l)$ in the Complex Plane $\mathbb{C}_{\varepsilon_{r_* \rightarrow \infty}}$

For the massive compact bodies with different values of the area radius of their surface the eigenvalue $\varepsilon_{r_* \rightarrow \infty}(n, s, l)$, as a function of $r_* \in (1, \infty)$, runs on some trajectory in the complex plane $\mathbb{C}_{\varepsilon_{r_* \rightarrow \infty}}$. Here we prove three simple properties of these trajectories. These properties are confirmed in the next section by numerical analysis of trajectories and illustrated in Figs. (3) and (4).

Proposition 1: *If the limit $r_* \rightarrow 1+0$ of the trajectory of $\varepsilon_{r_* \rightarrow \infty}(n, s, l)$ in the complex plane $\mathbb{C}_{\varepsilon_{r_* \rightarrow \infty}}$ exist, then we have:*

$$\lim_{r_* \rightarrow 1+0} \varepsilon_{r_* \rightarrow \infty}(n, s, l) = 0. \quad (3.18)$$

Proof: The eigenvalue $\varepsilon_{r_* \rightarrow \infty}(n, s, l)$ is obtained from the corresponding Eq. (3.17). Hence, its dependence on r_* is defined by the rhs of this equation.

The lhs of Eq. (3.17) must be nonzero and finite, because the solutions (2.13) and (2.14) are two complete sets of independent local solutions of the Regge-Wheeler equation.

Suppose that the limit (3.18) exists. According to the relations (2.9a) and (2.13b), the limit $r_* \rightarrow 1 + 0$ of the rhs of Eq. (3.17):

$$\lim_{r_* \rightarrow 1+0} e^{2i\varepsilon \ln(r_* - 1)} = \lim_{r_* \rightarrow 1+0} (e^{2i\Re(\varepsilon_{r_* \rightarrow \infty}(n, s, l)) \ln(r_* - 1)} e^{-2\Im(\varepsilon_{r_* \rightarrow \infty}(n, s, l)) \ln(r_* - 1)}) \quad (3.19)$$

does not exist if $\lim_{r_* \rightarrow 1+0} (\Re(\varepsilon_{r_* \rightarrow \infty}(n, s, l))) \neq 0$. If $\lim_{r_* \rightarrow 1+0} (\Re(\varepsilon_{r_* \rightarrow \infty}(n, s, l))) = 0$ and $\lim_{r_* \rightarrow 1+0} (\Im(\varepsilon_{r_* \rightarrow \infty}(n, s, l))) > 0$, the limit (3.19) is infinite. In the case $\lim_{r_* \rightarrow 1+0} (\Im(\varepsilon_{r_* \rightarrow \infty}(n, s, l))) < 0$ the limit (3.19) is zero. Hence, if a nonzero finite limit (3.19) exists, Eq. (3.18) must be fulfilled. \diamond

Proposition 2: *In the limit $r_* \rightarrow +\infty$ on the trajectory of $\varepsilon_{r_* \rightarrow \infty}(n, s, l)$ in the complex plane $\mathbb{C}_{\varepsilon_{r_* \rightarrow \infty}}$ we have:*

$$\lim_{r_* \rightarrow +\infty} \varepsilon_{r_* \rightarrow \infty}(n, s, l) = 0. \quad (3.20)$$

Proof: Using the expansion on $R_{\varepsilon, s, l}^{(\infty)\pm}(r_*)$ of type (2.16) for $R_{\varepsilon, s, l}^{(1)\pm}(r_*)$ in Eq. (3.17) and the properties (2.20), one easily obtains the limit $r_* \rightarrow +\infty$ of both sides of relation (3.17) in the form:

$$\lim_{r_* \rightarrow +\infty} \left(\frac{\Gamma_{\infty-}^{1+}(\varepsilon_{r_* \rightarrow \infty}(n, s, l), s, l)}{\Gamma_{\infty-}^{1-}(\varepsilon_{r_* \rightarrow \infty}(n, s, l), s, l)} \right) = \lim_{r_* \rightarrow +\infty} \left(\frac{\Gamma_{\infty+}^{1+}(\varepsilon_{r_* \rightarrow \infty}(n, s, l), s, l)}{\Gamma_{\infty+}^{1-}(\varepsilon_{r_* \rightarrow \infty}(n, s, l), s, l)} \right). \quad (3.21)$$

This means that in the limit $r_* \rightarrow +\infty$ the solutions $R_{\varepsilon, s, l}^{(1)\pm}(r)$ become linearly dependent. Formulae (2.13) show that this is possible only when equation (3.20) takes place. \diamond

Proposition 3: *The trajectory of eigenvalue $\varepsilon_{r_* \rightarrow \infty}(n, s, l)$ in the complex plane $\mathbb{C}_{\varepsilon_{r_* \rightarrow \infty}}$ has no cusps, i.e. the real part $\Re(\varepsilon_{r_* \rightarrow \infty}(n, s, l))$ and the imaginary part $\Im(\varepsilon_{r_* \rightarrow \infty}(n, s, l))$ can not have simultaneously extremum for finite values of $r_* \in (1, \infty)$.*

Proof: Let us introduce the short notation $g(\varepsilon) = \Gamma_{\infty-}^{1+}(\varepsilon, s, l)/\Gamma_{\infty-}^{1-}(\varepsilon, s, l)$ and $h(\varepsilon, r_*) = R_{\varepsilon, s, l}^{(1)+}(r_*)/R_{\varepsilon, s, l}^{(1)-}(r_*)$. Then Eq. (3.17), written down in the short form $g(\varepsilon) - h(\varepsilon, r_*) = 0$, defines implicitly the function $\varepsilon(r_*)$ in the general case when $\partial_\varepsilon(g(\varepsilon) - h(\varepsilon, r_*)) \neq 0$. For a derivative of the function $\varepsilon(r_*)$ one obtains $\partial_\varepsilon(g(\varepsilon) - h(\varepsilon, r_*)) \frac{d\varepsilon}{dr} = \partial h(\varepsilon, r_*) = -W(R_{\varepsilon, s, l}^{(1)+}(r_*), R_{\varepsilon, s, l}^{(1)-}(r_*)) / (R_{\varepsilon, s, l}^{(1)-}(r_*))^2$, where $W(R_{\varepsilon, s, l}^{(1)+}(r_*), R_{\varepsilon, s, l}^{(1)-}(r_*))$ denotes the corresponding Wronskian. Since $(R_{\varepsilon, s, l}^{(1)-}(r_*))^2 \neq \infty$ for finite $r_* \in (1, \infty)$, we can have $\frac{d\varepsilon}{dr}(r_*) = 0$ if, and only if $W(R_{\varepsilon, s, l}^{(1)+}(r_*), R_{\varepsilon, s, l}^{(1)-}(r_*)) = 0$. This contradicts to linear independence of the local solutions $R_{\varepsilon, s, l}^{(1)+}(r_*)$ and $R_{\varepsilon, s, l}^{(1)-}(r_*)$ for finite $r_* \in (1, \infty)$. \diamond

4 Numerical Calculation of Quasi-Normal Modes of Static Spherically Symmetric Objects

4.1 Transition Coefficients From Limit Procedures

As we have seen in the previous sections, for determination of QNM in simple models of compact objects we need to use the transition coefficients $\Gamma_{Y\pm}^{X\pm}(\varepsilon, s, l)$. Since these are not known explicitly, one has to apply more sophisticated methods for solving two-point boundary problems, instead of employing directly Eqs. (3.2) and (3.17).

In this section we present a new simple technique for calculation of quasi-normal modes of Schwarzschild black holes and massive spherically symmetric bodies, using directly the exact solutions of the Regge-Wheeler equation, found for the first time in the present article. We use our own computer code, written in Maple 10 package. There a pioneering implementation in computer algebra systems of the five Heun functions for complex values of argument and of corresponding parameters already exist. We use the numerically well studied case of Schwarzschild black holes to compare our results with the earlier ones, which were obtained by making use of two other numerical methods of Leaver and Andersson [7].

The basic idea of our new method is to use proper limit procedures for calculation of transition coefficients.

Let us consider some solution $R_{\varepsilon,s,l}(r)$ of the stationary Regge-Wheeler equation and let

$$R_{\varepsilon,s,l}(r) = C_{1+}R_{\varepsilon,s,l}^{(1)+}(r) + C_{1-}R_{\varepsilon,s,l}^{(1)-}(r) = C_{\infty+}R_{\varepsilon,s,l}^{(\infty)+}(r) + C_{\infty-}R_{\varepsilon,s,l}^{(\infty)-}(r) \quad (4.1)$$

present its expansions on the corresponding basic solutions (2.13) and (2.14). Then

$$C_{\infty\pm} = C_{1+}\Gamma_{\infty\pm}^{1+}(\varepsilon, s, l) + C_{1-}\Gamma_{\infty\pm}^{1-}(\varepsilon, s, l), \quad (4.2)$$

and we obtain the modulus of these constants using relations (2.20) in calculation of the following limits:

$$|C_{\infty+}| = \lim_{|r| \rightarrow +\infty} |e^{+i\varepsilon(r+\ln r)} R_{\varepsilon,s,l}(r)| : \text{ for } \arg(r) + \arg \varepsilon \in (0, \pi), \quad (4.3a)$$

$$|C_{\infty-}| = \lim_{|r| \rightarrow +\infty} |e^{-i\varepsilon(r-\ln r)} R_{\varepsilon,s,l}(r)| : \text{ for } \arg(r) + \arg \varepsilon \in (-\pi, 0). \quad (4.3b)$$

In addition, it becomes clear from asymptotics (2.19) that in the limit (4.3b) we have the steepest descent, if and only if $\arg(r) + \arg \varepsilon = -\frac{\pi}{2} / \text{mod } 2\pi$. This direction is the optimal one for numerical calculations of the above limits, as we shall see below.

This way we can obtain the needed information about transition coefficients $\Gamma_{\infty\pm}^{1\pm}(\varepsilon, s, l)$, using any solution with known constants $C_{1\pm}$. Alternatively, we can impose the corresponding boundary conditions directly on the modulus $|C_{\infty\pm}|$, calculated via the limits (4.3).

4.2 QNM of Schwarzschild Black Holes

Already in a first calculation the QNM frequencies, made by Chandrasekhar and Detweiler [7] the following difficulties were recognized: It is hard to nullify numerically the coefficient in front of the solution $R_{\varepsilon,s,l}^{(\infty)-}(r)$ (see Eq. (3.2)), which is small on the left of the infinite point on the *real* axes. This happens because it is hard to distinguish the small solution $R_{\varepsilon,s,l}^{(\infty)-}(r)$ in the presence of unavoidable numerical errors in the solution

$R_{\varepsilon,s,l}^{(\infty)+}(r)$, which is dominant in this domain. Therefore, much more sophisticated methods, like Leaver's continuous fraction method and Andersson's phase amplitude method for accurate calculations of QNM spectrum, were invented successfully, see references in [7]. This way were obtained the known most accurate values for QNM frequencies.

For example, in Andersson's article, among many others, one can find the value of the basic quasi-normal mode of gravitational waves: $\varepsilon_{1\sim\infty}(0, 2, 2)_{\text{Andersson}} = 0.747343368 + i 0.17792463$.

Using the Leaver's method on modern computers, it is easy to find several more figures: $\varepsilon_{1\sim\infty}(0, 2, 2)|_{\text{Leaver}} = 0.747343368836 + i 0.177924631377$ for the same mode⁷.

Since today we have at our disposal a possibility to calculate the canonical solution (2.3) of Heun's equation in the complex domain of variables using Maple 10, we are able to turn back to the idea of solving numerically Eq. (3.2)), in a properly modified way, which overcomes the difficulty of Chandrasekhar-Detweiler method. Our solution is based on the limit procedure (4.3b) which shows that in the direction $\arg(r) + \arg \varepsilon = -\frac{\pi}{2}$ the solutions interchange their roles. The former small solution becomes a dominant one. Taking into account expressions (2.13), one easily obtains the following form of the equation for for QNM spectrum of Schwarzschild black holes:

$$\lim_{|r|\rightarrow+\infty} \left| r^{s+1} \text{HeunC} \left(-2i\varepsilon, 2i\varepsilon, 2s, -2\varepsilon^2, 2\varepsilon^2 + s^2 - l(l+1), 1 - |r|e^{i(\frac{\pi}{2}+\arg(\varepsilon))} \right) \right| = 0. \quad (4.4)$$

In a numerical treatment of the problem we replace the last limiting procedure with calculation at some finite point $r_\infty \gg 1$, i.e. we use the equation:

$$\left| (r_\infty)^{s+1} \text{HeunC} \left(-2i\varepsilon, 2i\varepsilon, 2s, -2\varepsilon^2, 2\varepsilon^2 + s^2 - l(l+1), 1 - r_\infty e^{i(\frac{\pi}{2}+\arg(\varepsilon))} \right) \right| = 0. \quad (4.5)$$

We apply the complex plot abilities of Maple 10 to find a relatively small vicinity of the complex roots of this equation. Then we justify their values to the desired precision using a direct check of the place of the corresponding root in the complex plane \mathbb{C}_ε and/or by Muller's method for finding of complex roots [10].

The results are shown in the Tables 2, 3, and 4. In the Table 2 the results of our numerical calculations for the first five eigenvalues are presented. We see an excellent agreement with the most accurate values, published up to now by Andersson [7].

The Table 3 shows that using high precision calculations with Eq. (4.5) one can produce the value of $\varepsilon_{1\sim\infty}(0, 2, 2)$ up to more figures – here up to 12 figures. This consideration inspires confidence in our new method for calculation of QNM. As seen from Table 3, with our Maple 10 computer code we obtain the right 9 figures already in 64 digits calculations. This gives us more confidence in the results for next several eigenvalues, obtained using the same method and shown in Table 2.

In the Table 4 we show the deviations of the values of the basic eigenvalue $\varepsilon_{1\sim\infty}(0, 2, 2)$, obtained by our method for different r_∞ , with respect to the corresponding value for $r_\infty = 100$ and for 32 digits calculations.

⁷The author is deeply indebted to prof. Kostas Kokkotas for permission to use his computer code for calculation of this value by Leaver's method.

$n = 0$	0.747343368 + i 0.177924631
$n = 1$	0.693421994 + i 0.547829750
$n = 2$	0.602106909 + i 0.956553966
$n = 3$	0.503009924 + i 1.410296405
$n = 4$	0.415029159 + i 1.893689781

Table 2: The first five eigenvalue for 64 digit calculations and for $r_\infty = 20$.

32	0.747343368602 + i 0.177924631717
64	0.747343368782 + i 0.177924631969
128	0.747343368864 + i 0.177924631732
256	0.747343368836 + i 0.177924631360

Table 3: The basic eigenvalue for higher number of digits (given in the first column) calculations (no rounding) and for $r_\infty = 20$.

As we see, the calculation of the eigenvalue $\varepsilon_{1\leftarrow\infty}(0, 2, 2)$, based on equation (4.5), is not very sensitive to the choice of r_∞ and for $r_\infty \geq 20$ it gives a stable right result up to seven figures for 32 digits calculations. A simple look on the Table 4 shows that the deviations have no systematic nature and may demonstrate instabilities (after the first seven figures) of Maple 10 calculations with 32 digits precision.

4.3 QNM of Massive Compact Body

Applying the limit procedure (4.3b) to our simple model of massive compact body, described in Section 3.4, we obtain the following equation for the corresponding QNM:

$$\begin{aligned}
 & \left| \lim_{|r| \rightarrow +\infty} \left(e^{2i*\varepsilon \ln(|r|e^{-i(\pi/2+\arg(\varepsilon))}-1)} \times \right. \right. \\
 & \left. \left. \frac{\text{HeunC}(-2i\varepsilon, +2i\varepsilon, 2s, -2\varepsilon^2, 2\varepsilon^2+s^2-l(l+1), 1-|r|e^{-i(\pi/2+\arg(\varepsilon))})}{\text{HeunC}(-2i\varepsilon, -2i\varepsilon, 2s, -2\varepsilon^2, 2\varepsilon^2+s^2-l(l+1), 1-|r|e^{-i(\pi/2+\arg(\varepsilon))})} \right) - \right. \quad (4.6) \\
 & \left. e^{2i*\varepsilon \ln(r_*-1)} \times \frac{\text{HeunC}(-2i\varepsilon, +2i\varepsilon, 2s, -2\varepsilon^2, 2\varepsilon^2+s^2-l(l+1), 1-r_*)}{\text{HeunC}(-2i\varepsilon, -2i\varepsilon, 2s, -2\varepsilon^2, 2\varepsilon^2+s^2-l(l+1), 1-r_*)} \right| = 0.
 \end{aligned}$$

The numerical treatment of this problem is the same as in the previous Subsection: we once more replace the limiting procedure with calculation at some finite point $r_\infty \gg 1$,

10	-.17e-8 - i .211e-7	100	0 + i 0
20	-.90e-8 - i .106e-7	200	.252e-7 - i .141e-7
30	-.96e-8 - i .105e-7	300	-.156e-7 + i .204e-7
40	-.65e-8 - i .82e-8	500	.2007e-6 - i .3180e-6
50	-.103e-7 - i .160e-7	1000	-.785e-7 - i .3198e-6
80	-.94e-8 - i .50e-8	1500	.2680e-6 - i .21134e-5

Table 4: The numerical results for 32 digit calculations of $\varepsilon_{1\sim\infty}(0, 2, 2)$ for different values of r_∞ (given in the first and in the third column). In this Table we present only the deviations from the value $\varepsilon_{1\sim\infty}(0, 2, 2)|_{100} = 0.747343377577 + i 0.177924642293$, obtained for $r_\infty = 100$.

i.e. we use the equation:

$$\left| e^{2i*\varepsilon \ln(r_\infty e^{-i(\pi/2+\arg(\varepsilon))}-1)} \times \frac{HeunC(-2i\varepsilon, +2i\varepsilon, 2s, -2\varepsilon^2, 2\varepsilon^2+s^2-l(l+1), 1-r_\infty e^{-i(\pi/2+\arg(\varepsilon))})}{HeunC(-2i\varepsilon, -2i\varepsilon, 2s, -2\varepsilon^2, 2\varepsilon^2+s^2-l(l+1), 1-r_\infty e^{-i(\pi/2+\arg(\varepsilon))})} - \right. \\ \left. e^{2i*\varepsilon \ln(r_*-1)} \times \frac{HeunC(-2i\varepsilon, +2i\varepsilon, 2s, -2\varepsilon^2, 2\varepsilon^2+s^2-l(l+1), 1-r_*)}{HeunC(-2i\varepsilon, -2i\varepsilon, 2s, -2\varepsilon^2, 2\varepsilon^2+s^2-l(l+1), 1-r_*)} \right| = 0 \quad (4.7)$$

and apply our own computer codes, written in Maple 10, for finding its roots. The results are shown in Fig. 3 and Fig. 4.

5 Conclusion

In the present article we have solved some mathematical problems related to exact solution of the Regge-Wheeler equation. Since the obtained results and possible further developments were described in detail in the basic text, in the concluding remarks we will comment on their eventual physical significance and some open problems.

In the present article we do not establish a definite relation between the spectrum of the problem with Dirichlet's boundary condition at the surface of the spherically symmetric body and the corresponding spectrum of more realistic models of relativistic stars [9]. The simple comparison of the published numerical results for relativistic stars with our results in Figs. 3, 4 shows that the complex eigenvalues of star's axial modes are placed in a complicated way in the domains, separated by the trajectories of QNM eigenvalues $\varepsilon_{r_*\sim\infty}(n, s, l)$, which belong to the simple model of massive compact objects, studied here for the first time⁸. One may hope that further investigation of this problem will help our understanding of QNM of compact matter objects.

⁸The author is grateful to unknown referee for its suggestion to consider such comparison.

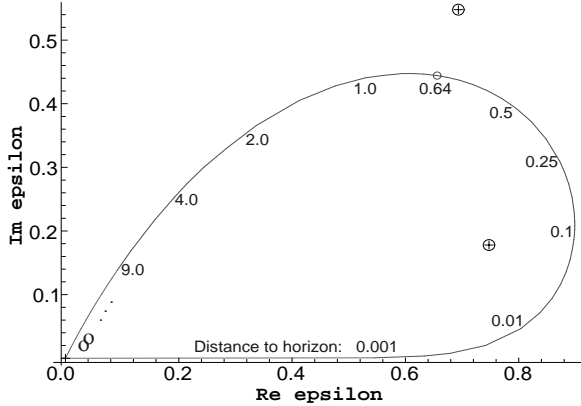


Figure 3: The complex trajectory of the basic eigenvalue $\varepsilon_{r_* \rightarrow \infty}(0, 2, 2)$ of QNM of compact massive body as a function of the distance $d = r_* - 1 > 0$ of the body's surface to the horizon (in units $2M$). For comparison purposes, the first two eigenvalues of QNM for Schwarzschild black holes with the same mass M are shown, using the circles with crosses. The origin of the complex plane \mathbb{C}_ε is marked by a small cross. It presents simultaneously the event horizon (where the trajectory begins) and the physical infinity (where the trajectory ends). The small circle on the trajectory denotes the position of the maximum of the effective potential $V(r)$.

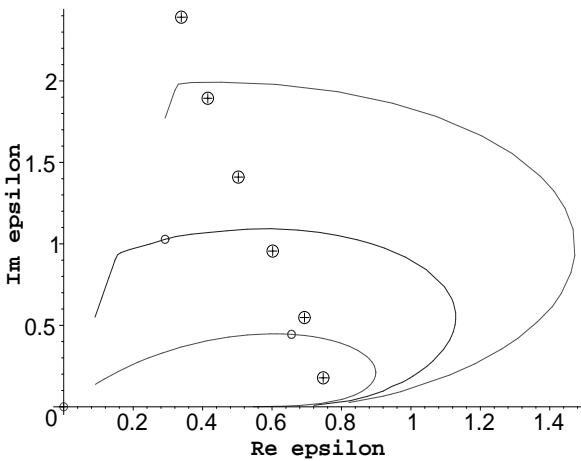


Figure 4: The trajectories in the complex plane \mathbb{C}_ε of the first three eigenvalues: $\varepsilon_{r_* \rightarrow \infty}(0, 2, 2), \varepsilon_{r_* \rightarrow \infty}(1, 2, 2)$ and $\varepsilon_{r_* \rightarrow \infty}(2, 2, 2)$ of QNM of massive compact body. For comparison purposes, the first six eigenvalues of QNM for Schwarzschild black holes with the same mass M are shown, using the circles with crosses. The small circles on the trajectories denote the corresponding positions of the maximum of effective potential $V(r)$.

A more realistic model for real spherically symmetric bodies may be obtained considering as a boundary condition a partial reflection and partial penetration of the waves through the body's surface. In the present article we have considered only the two extreme cases for reflection coefficient: $R = 0$ – for the black holes and $R = 1$ – for our simple model of bodies. It is interesting to know will it be possible to connect continuously these two cases, introducing a coefficient of reflection $R \in [0, 1]$, or the difference in the boundary conditions is an insuperable obstacle for this.

In the near future our results may be useful for the planned observations of gravitational waves emitted by or spreading around existing real compact objects. These results may help to clarify the physical nature of the observed very heavy and very compact dark objects in the universe. Our consideration gives a unique possibility for a *direct* experimental test of the existence of space-time *holes*. The study of spectra of the corresponding waves, propagating around compact dark objects, may give indisputable evidences, whether there is space-time hole inside such an invisible object.

Similar results can be obtained for electromagnetic, spinor and scalar waves in the external Schwarzschild gravitational field of compact objects. A further study of these phenomena is an important physical problem and may offer practical physical criteria for experimental distinction of the two completely different hypothetical models:

- 1) The model of space-time black holes; and
- 2) Different new models of very compact dark objects, made of *real*, or of some *hypothetical* matter [11].

The present-day astrophysical observations still are not able to make difference between these two cases. The only real observational fact is that we see very compact and very massive objects which show up *only* due to their *external* strong gravitational field. An actual theoretical problem is to find a convincing model for description of these already observed compact dark objects and the criteria for experimental verification of a model like this. We hope that the present article is a step in this direction.

Acknowledgments

The author is grateful to the High Energy Physics Division, ICTP, Trieste, for the hospitality and for the nice working conditions during his visit in the autumn of 2003. There the idea of the present article was created. The author is grateful to the JINR, Dubna, too, for the priority financial support of the present article, for the hospitality and for the good working conditions during his three months visits in 2003, 2004 and 2005, when the study was performed in detail. This article also was supported by the Scientific Found of Sofia University, and by its Foundation "Theoretical and Computational Physics and Astrophysics".

I wish to acknowledge the participants in the scientific seminars of ICTP -Trieste, BLTF of JINR - Dubna and INRNE - Sofia for stimulating discussions of the basic ideas, methods, and results of the present article.

I am deeply indebted to prof. Kostas Kokkotas for the useful discussions and for providing a simple FORTRAN computer code for calculations of the first several QNM of Schwarzschild black holes by Leaver's method. This code, being produced and used in earlier studies in his group in Thessaloniki was kindly e-mailed by prof. Kokkotas to our Joint Group on Gravity and Astrophysics in Sofia. The comparison of our Maple 10 results

for Schwarzschild black holes with the corresponding high precision results, obtained by the Leaver's method, increases substantially our confidence in the new method, developed in the present article.

I wish to express my thanks to prof. Michail Todorov – for help and discussions of numerical techniques used in the present article, to prof. Nils Andersson – for sending me a copy of his article, cited in [7], to prof. Matt Visser for drawing my attention to five more references, included in [11], to prof. Paweł Mazur – for adding a new reference and corrections in [11], and to two unknown referees for their extremely useful suggestions for improvements of the article and for help in the references.

6 Appendix: General Properties of the Complex Current and Some Important Consequences

6.1 General Properties of the Complex Curl

At first glance the Regge-Wheeler eigenvalue problem seems to be quite similar to the Schrödinger eigenvalue problem in quantum mechanics. There one considers usually *real* eigenvalues of the energy operator. The last assumption yields existence of a conserved *real* current. This current describes an essential physical information about the solutions of the problem. We were not able to find in the literature a proper investigation of the properties of the current in RW problem with *complex* eigenvalues ε . Therefore in this Appendix we define the corresponding *complex* current, study its basic properties and derive some consequences, which are essential for our article.

In the case of $\varepsilon \in \mathbb{C}$, $\varepsilon_R > 0$, $\varepsilon_I \neq 0$, and $V \in \mathbb{R}$ the stationary RW equation (1.2) for $R = X + iY = |R|e^{i\varphi}$ is equivalent to the real system of 4th order ordinary differential equations:

$$X'' = (V - \xi)X + \eta Y, \quad Y'' = (V - \xi)Y - \eta X, \quad (6.1)$$

where the prime denotes differentiation with respect to RW tortoise variable x and $\varepsilon^2 = \varepsilon_R^2 - \varepsilon_I^2 + 2i\varepsilon_R\varepsilon_I = \xi + i\eta$. In the case $\eta \neq 0$ this system does not split into two independent differential equations of 2nd order and in addition we obtain:

$$\xi = V + \frac{(X')^2 + (Y')^2}{X^2 + Y^2} - \frac{(XX' + YY')'}{X^2 + Y^2}, \quad \eta = \frac{(YX' - XY')'}{X^2 + Y^2}. \quad (6.2)$$

Despite of the above fact, for $\eta \neq 0$ the system (6.1) is equivalent to 2nd order system of *real* nonlinear differential equations (see, for example, the article by S. Chandrasekhar and S. L. Detweiler in [7]):

$$u'_R = \eta - 2u_R u_I, \quad u'_I = u_R^2 - u_I^2 + V - \xi, \quad (6.3)$$

with boundary conditions at infinity: $u_R(\infty) = \varepsilon_R > 0$, $u_I(\infty) = \varepsilon_I > 0$ – for QNM. This phenomenon turns to be possible since two of the arbitrary real constants in the general solution of the system (6.1) are actually not essential, entering inessential complex constant multiplier of form $R_* = |R_*|e^{i\varphi_*}$ in the solution R of the RW eq. (1.2). This constant always can be chosen to be equal to 1. To obtain Eqs. (6.3) we use the substitution:

$$R = e^{-i \int u(x) dx} = e^{-i \int u_R(x) dx} e^{\int u_I(x) dx}, \quad (6.4)$$

where

$$u = u_R + iu_I = i\frac{R'}{R} = i\frac{R'\bar{R}}{|R|^2} = \frac{j_R + i j_I}{|R|^2}. \quad (6.5)$$

This way we introduce a *complex* current $j = j_R + i j_I = u_R|R|^2 + i u_I|R|^2$ in the RW problem. Using the Eqs. (6.1), it is easy to obtain the following relations:

$$\begin{aligned} j_R &= XY' - XY', \quad j'_R = \eta(X^2 + Y^2), \quad j''_R = 2\eta(XX' + YY'), \\ j'''_R &= 2\eta((X')^2 + (Y')^2) + 2\eta(V - \xi)(X^2 + Y^2), \end{aligned} \quad (6.6)$$

and the 4th order differential equation for the real part j_R of the complex current

$$j_R^{IV} = 4(V - \xi)j''_R + V'j'_R + 4\eta^2j_R. \quad (6.7)$$

One sees that for $\eta \neq 0$:

- i) The complex current j is not conserved, i.e. $j_R \neq \text{const}$ and $j_I \neq \text{const}$.
- ii) Since $j_I = \frac{1}{2\eta}j''_R = XX' + YY'$, in the imaginary part j_I of the current j there is no independent information.
- iii) In addition $|R|^2 = j'_R/\eta$, $\varphi' = -\eta j_R/j'_R$. Hence, the real component j_R of the complex current j contains all essential information for the RW problem and the Eq. (6.7) can replace RW one (1.2) in all considerations.

It is easy to obtain the first integral $\frac{1}{4}((j'_R)^2)'' - \frac{3}{4}(j''_R)^2 - (V - \xi)(j'_R)^2 - \eta^2j_R^2 = \text{const}$ of the Eq. (6.7). The constant value of this integral turns to be one of the two inessential constants in the general solution of the Eq. (6.7). Without loss of generality we can assume that this constant equals zero. Then the real part j_R obeys 3th order differential equation:

$$\frac{1}{4}((j'_R)^2)'' = \frac{3}{4}(j''_R)^2 + (V - \xi)(j'_R)^2 + \eta^2j_R^2 \quad (6.8)$$

Using the substitution $j_R = \exp(\eta \int u_R(x)dx)$ one can exclude the second inessential constant in the general solution of the Eq. (6.7), lowering once more its order. Thus we obtain the single 2nd order differential equation:

$$\frac{1}{2} \left(\frac{\eta - u'_R}{u_R} \right)' = -\frac{1}{4} \left(\frac{\eta - u'_R}{u_R} \right)^2 + u_R^2 + V - \xi, \quad (6.9)$$

which can be derived directly from the system (6.3), too. The last observation supports our choice of the zero value for the first integral of Eq. (6.7).

At the end let us introduce functions $R_{\leftarrow} = \frac{1}{2}(R + \frac{1}{ik}R')$, $R_{\rightarrow} = \frac{1}{2}(R - \frac{1}{ik}R')$ putting

$$R = R_{\leftarrow} + R_{\rightarrow}, \quad R' = ik(R_{\leftarrow} - R_{\rightarrow}). \quad (6.10)$$

Here $k = \sqrt{\varepsilon^2 - V}$ and we suppose to choose the branch of the square root for which we have $k = \varepsilon$ when $V = 0$. Now we obtain

$$j = k(|R_{\rightarrow}|^2 - |R_{\leftarrow}|^2), \quad (6.11)$$

precisely as in the real case $\varepsilon_I = 0$.

The complex functions R_{\rightarrow} and R_{\leftarrow} obey the 2nd order system

$$\begin{pmatrix} R_{\leftarrow} \\ R_{\rightarrow} \end{pmatrix}' = \hat{H} \begin{pmatrix} R_{\leftarrow} \\ R_{\rightarrow} \end{pmatrix}, \quad \hat{H} = k \begin{pmatrix} 1 & 0 \\ 0 & 1 \end{pmatrix} + i \frac{k'}{2k} \begin{pmatrix} 1 & -1 \\ -1 & 1 \end{pmatrix}, \quad (6.12)$$

which shows that at the points where $V' = 0$ these functions describe waves which run to the right and to the left, correspondingly. If, in addition, $V = 0$, then $j_{\rightarrow} = \varepsilon_R|R_{\rightarrow}|^2$, $j_{\leftarrow} = -\varepsilon_R|R_{\leftarrow}|^2$.

6.2 Special Properties of the Current in the Case of Compact Body with Dirichlet's Boundary Condition at the Surface

In the simple model of compact body with Dirichlet's boundary condition (3.12) one has $R(x_*) = 0$, $R'_* = R'(x_*) \neq 0$. As a result in vicinity of the point x_* one obtains the following series expansions with respect to the difference $\Delta x = x - x_*$:

$$R(x) = R'_* \left(\Delta x + \frac{1}{6}(V_* - \varepsilon^2)\Delta x^3 + \frac{1}{12}V'_*\Delta x^4 + \mathcal{O}_6(\Delta x) \right), \quad (6.13)$$

$$u_R(x) = \frac{\eta}{3}\Delta x + \mathcal{O}_3(\Delta x), \quad (6.14a)$$

$$u_I(x) = \frac{1}{\Delta x} + \frac{1}{3}(V_* - \xi)\Delta x + \frac{1}{4}V'_*\Delta x^2 + \mathcal{O}_3(\Delta x); \quad (6.14b)$$

$$j_R(x) = \eta|R'_*|^2 \left(\frac{1}{3}\Delta x^3 + \frac{1}{15}(V_* - \xi)\Delta x^5 + \frac{1}{36}V'_*\Delta x^6 + \mathcal{O}_7(\Delta x) \right), \quad (6.15a)$$

$$j_I(x) = |R'_*|^2 \left(\Delta x + \frac{2}{3}(V_* - \xi)\Delta x^3 + \frac{5}{6}V'_*\Delta x^4 + \mathcal{O}_5(\Delta x) \right); \quad (6.15b)$$

and the two equivalent sets of integral representations:

$$u_R(x) = \eta|R(x)|^{-2} \int_{x_*}^x |R(x)|^2 dx, \quad (6.16a)$$

$$u_I(x) = |R(x)|^{-1} \int_{x_*}^x (|u_R(x)|^2 + (V(x) - \xi)|R(x)|) dx + \frac{|R'_*|}{|R(x)|}, \quad (6.16b)$$

and

$$j_R(x) = \eta \int_{x_*}^x |R(x)|^2 dx, \quad (6.17a)$$

$$j_I(x) = \int_{x_*}^x (|R'(x)|^2 + V(x)|R(x)|^2) dx - \xi \int_{x_*}^x |R(x)|^2 dx. \quad (6.17b)$$

With the help of the Eq. (6.17a) the Eq. (6.17b) can be rewritten in the form

$$\xi j_R(x) + \eta j_I(x) = \eta \int_{x_*}^x (|R'(x)|^2 + V(x)|R(x)|^2) dx. \quad (6.18)$$

Now we obtain the following additional properties of the solutions of RW equation for compact body with Dirichlet's boundary condition at its surface:

1. NM do not exist for $\eta \neq 0$ in the Dirichlet's boundary problem (3.12) . Indeed, since for NM $R(\infty) = 0$, one must have for them $0 = j_R(\infty) = \eta \int_{x_*}^{\infty} |R(x)|^2 dx$. Hence, $R(x) \equiv 0$ for $x \in [x_*, \infty)$ and we will have a trivial zero-solution.

2. For QNM we have $\eta > 0$, because of our assumption $\varepsilon_R > 0$. Then we obtain the following properties of QNM in this problem:

i) The solutions $R(x)$ and the current $j_R(x)$ cannot have other zeros x_0 , different from x_* . Indeed, if $R(x_0)=0$, then $0 = j_R(x_0) = \eta \int_{x_*}^{x_0} |R(x)|^2 dx \geq 0$ leads to $x_0 \equiv x_*$ for any nontrivial solution $R(x) \neq 0$.

ii) If $\varepsilon_I \geq \varepsilon_R$, then $\xi \leq 0$ and Eq. (6.17b) shows that $j_I(x) > 0$ and $j''_r > 0$ for any $x \in (x_*, \infty)$.

iii) Oscillations of $j_I(x)$ (and j''_r) around the zero value:

From Eq. (6.17b) we see, that $j_I(x)$ (and $j''_R(x) = 2\eta j_I(x)$) can have a second zero, besides x_* , if and only if $\varepsilon_I < \varepsilon_R$, i.e. when $\xi > 0$. Then, since $\lim_{x \rightarrow \infty} j_R(x) = \lim_{x \rightarrow \infty} (u_R(x)|R(x)|^2) = +\infty$, the current $j_R(x)$ must have at list one more (third) zero in the interval $[x_*, \infty)$. This way we see that in general case for $\xi > 0$ the imaginary part $j_I(x)$ of the complex current has an odd number (≥ 1) of zeros and its derivative $j'_I(x)$ has an even number (≥ 0) of zeros in the interval $[x_*, \infty)$.

iv) From Eq. (6.18) for $x > x_*$ we obtain the inequality:

$$j_I(x) \geq \frac{1}{2} \left(\frac{\varepsilon_I}{\varepsilon_R} - \frac{\varepsilon_R}{\varepsilon_I} \right) j_R(x). \quad (6.19)$$

References

- [1] T. Regge, J. A. Wheeler, 1957, Phys. Rev. **108**, 1063.
S. Chandrasekhar, 1983, *The Mathematical Theory of Black Holes*, Oxford University Press, Oxford.
- [2] R. M. Corless, G. H. Gonnet, D. E. G. Hare, D. J. Jeffrey, D. E. Knuth, 1996, Advances in Comp. Math. **5**, 329.
- [3] V. Ferrari, 1995, in *Proc. of 7-th Marcel Grossmann Meeting*, ed, R. Ruffini, M. Kaiser, Singapoore, World Scientific; and 1998, in *Black Holes and Relativistic Stars*, ed. R. Wald, Univ. Chicago Press.
K. D. Kokkotas, B. G. Schmidt, 1999, Living Rev. Relativity **2**, 2.
H-P. Nollert, 1999, Class. Quant. Grav. **16**, R159.
E. Berti, 2004, *Black hole quasinormal modes: hints of quantum gravity?*, gr-qc/0411025.
- [4] M. F. Manning, 1935, Phys. Rev. **48**, 161.
- [5] K. Heun, 1889, Math. Ann. **33**, 161.
H. Bateman, A. Erdélyi, 1955, Higher Transcendental Functions, Vol. 3, Mc Grow-Hill Comp., INC.

A. Decarreau, M. Cl. Dumont-Lepage, P. Maroni, A. Robert, A. Roneaux, 1978, Ann. Soc. Buxelles, **92**, 53.

A. Decarreau, P. Maroni, A. Robert, 1978, Ann. Soc. Buxelles, **92**, 151. 1995, Heun's Differential Equations, ed. A. Roneaux, Oxford Univ. Press.

S.Y. Slavyanov and W.Lay, 2000, "Special Functions, A Unified Theory Based on Singularities", Oxford Mathematical Monographs.

R. S. Maier, 2004, *The 192 Solutions of Heun Equation*, math.CA/0408317.

[6] C. V. Vishveshwara, 1970, Phys. Rev. D**1**, 2870.

J. M. Steward, 1975, Proc. R. Soc. A**344**, 65.

R. M. Wald, 1979, J. Math. Phys., **20**, 1056.

[7] S. Chandrasekhar, S. L. Detweiler, 1975, Proc. R. Soc. London, A**344**, 441.

E. W. Leaver, 1985, Proc. R. Soc. London, A**402**, 285.

N. Andersson, 1992, Proc. R. Soc. London, A**439**, 47.

[8] G. T. Horowitz, V. E. Hubeny, 2000, Phys. Rev. D**62**, 024027.

[9] S. Chandrasekhar, V. Ferrari, 1991, Proc. R. Soc. A**432**, 247.

S. Chandrasekhar, V. Ferrari, 1991, Proc. R. Soc. A**434**, 449.

M. Leins, H. P. Nollert, M. H. Soffel, 1993, Phys. Rev. D**48**, 3467.

K. D. Kokkotas, MNRAS 1994, **268**, 1015.

K. D. Kokkotas, MNRAS 1995, **277**, 1599.

O. Behar, E. Berti, V. Ferrari, 1999, MNRAS, **310**, 797.

[10] W. H. Press, S. A. Teukolsky, W. T. Wetterling, B. P. Flannery, 1992, *Numerical Recipes in Fortran 77*, Vol. 1, Second Edition, Cambridge University Press.

[11] P. A. M. Dirac, 1962, Proc. Roy Soc. (London), A**270**, 354; and 1964, Conference in Warszawa and Jablonna, L. Infeld ed., Gauthier-Villars, Paris, pp. 163-175.

A. Cabo, E. Ayon-Beato, 1999, Int. J. Mod. Phys. A**14**, 2013.

G. Chapline, E. Hohlfeld, R. B. Laughlin, D. Santiago, 2001, Phil. Mag. D **81**, 235.

E. Mottola, P. Mazur, 2001, *Gravitational Condensate Stars: An Alternative to Black Holes*, gr-qc/0109035.

G. Chapline, R. B. Laughlin, D. Santiago, 2002, in *Artificial black holes*. ed. M. Novello, M. Visser, and G. Volovik, World Sci. Singapoore.

G. Chapline, E. Hohlfeld, R. B. Laughlin, D.I. Santiago, 2003, Int. J. Mod. Phys. A**18**, 3587.

P. O. Mazur, E. Mottola, 2004, Proc. Nat. Acad. Sci., **111**, 9546.

J. Barbierii, G. Chapline, 2004, Phys. Lett. B**590**, 8.

M. Visser, D. L. Wiltshire, 2004, Class. Quant. Grav., **21**, 1135.

P. P. Fiziev, 2003, *Gravitational Field of Massive Point Particle in General Relativity*, gr-qc/0306088; Abdus Salam ICTP, Trieste, Italy: preprint IC/2003/122.

P. P. Fiziev, 2004, *On the Solutions of Einstein Equations with Massive Point Source*, in Proceedings of the Conference Gravity, Astrophysics and strings at Black Sea 2004, St. Kliment Ohridski University Press, Sofia, 2005, p. 70; gr-qc/0407088.

G. Chapline, 2005, *Dark Energy Stars*, astro-ph/0503200.

C. Cattoen, T. Faber, M. Visser, 2005, *Gravastars must have anisotropic pressures*, gr-qc/0505137.

F. S. N. Lobo, 2005, *Stable Dark Energy Stars*, gr-qc/0508115.

A. DeBenedictis, D. Horvat, S. Ilijic, S. Kloster, K. S. Viswabathan, 2005, *Gravastar Solutions with Continuous Pressures and Equation of State*, gr-qc/0511097.